Communication

Serological Test to Determine Exposure to SARS-CoV-2: ELISA Based on the Receptor-Binding Domain of the Spike Protein (S-RBD$_{N318-V510}$) Expressed in *Escherichia coli*

Alan Roberto Márquez-Ipiña [1,†], Everardo González-González [2,†], Iram Pablo Rodríguez-Sánchez [3,4], Itzel Montserrat Lara-Mayorga [1,5], Luis Alberto Mejía-Manzano [1], Mónica Gabriela Sánchez-Salazar [2], José Guillermo González-Valdez [1], Rocio Ortiz-López [6], Augusto Rojas-Martínez [6], Grissel Trujillo-de Santiago [1,5,*] and Mario Moisés Alvarez [1,2,*]

1   Centro de Biotecnología-FEMSA, Tecnologico de Monterrey, Monterrey CP 64849, NL, Mexico; alanmarquez_86@hotmail.com (A.R.M.-I.); montserrat.lara@tec.mx (I.M.L.-M.); alberto.mejia.m@tec.mx (L.A.M.-M.); jose_gonzalez@tec.mx (J.G.G.-V.)
2   Departamento de Bioingeniería, Tecnologico de Monterrey, Monterrey CP 64849, NL, Mexico; dnarnaprot@gmail.com (E.G.-G.); a01054898@itesm.mx (M.G.S.-S.)
3   Laboratorio de Fisiología Molecular y Estructural, Facultad de Ciencias Biológicas, Universidad Autónoma de Nuevo León, San Nicolas de los Garza CP 66455, NL, Mexico; iram.rodriguezsa@uanl.edu.mx
4   Alfa Medical Center, Guadalupe CP 67100, NL, Mexico
5   Departamento de Ingeniería Mecatrónica y Eléctrica, Tecnologico de Monterrey, Monterrey CP 64849, NL, Mexico
6   Tecnologico de Monterrey, Escuela de Medicina y Ciencias de la Salud, Monterrey CP 64718, NL, Mexico; rortizl@tec.mx (R.O.-L.); augusto.rojas.mtz@tec.mx (A.R.-M.)
*   Correspondence: grissel.trujillo@tec.mx (G.T.-d.S.); mario.alvarez@tec.mx (M.M.A.)
†   These authors contributed equally to this work.

Abstract: Massive worldwide serological testing for SARS-CoV-2 is needed to determine the extent of virus exposure in a particular region, the ratio of symptomatic to asymptomatic infected persons, and the duration and extent of immunity after infection. To achieve this, the development and production of reliable and cost-effective SARS-CoV-2 antigens is critical. We report the bacterial production of the peptide S-RBD$_{N318-V510}$, which contains the receptor-binding domain of the SARS-CoV-2 spike protein (region of 193 amino acid residues from asparagine-318 to valine-510) of the SARS-CoV-2 spike protein. We purified this peptide using a straightforward approach involving bacterial lysis, his-tag-mediated affinity chromatography, and imidazole-assisted refolding. The antigen performances of S-RBD$_{N318-V510}$ and a commercial full-length spike protein were compared in ELISAs. In direct ELISAs, where the antigen was directly bound to the ELISA surface, both antigens discriminated sera from non-exposed and exposed individuals. However, the discriminating resolution was better in ELISAs that used the full-spike antigen than the S-RBD$_{N318-V510}$. Attachment of the antigens to the ELISA surface using a layer of anti-histidine antibodies gave equivalent resolution for both S-RBD$_{N318-V510}$ and the full-length spike protein. Results demonstrate that ELISA-functional SARS-CoV-2 antigens can be produced in bacterial cultures, and that S-RBD$_{N318-V510}$ may represent a cost-effective alternative to the use of structurally more complex antigens in serological COVID-19 testing.

Keywords: SARS-CoV-2; COVID-19; ELISA; serological testing; spike; receptor binding domain; *Escherichia coli*; antigen

1. Introduction

Severe acute respiratory syndrome coronavirus 2 (SARS-CoV-2), the causal agent of the coronavirus disease 19 (COVID-19), has infected more than 95 million people [1], at the time of this writing. Never before in contemporary history has humankind faced an infectious disease at this scale. In response to this unprecedented challenge, a vast number

of methods to screen for SARS-CoV-2 infection have been proposed [2]. These diagnostic methods are based on the identification of SARS-CoV-2 antigens, the amplification of SARS-CoV-2 nucleic acids [3,4], or the detection of anti-SARS-CoV-2 antibodies [5]. Antigen-based methods are particularly useful for massive screening efforts: their cost is relatively low, they are easily implementable and portable, and their specificity is high (~100%); however, their sensitivity is often lower than that of amplification-based methods (~30–81%) [6–8]. Amplification-based methods are highly accurate (sensitivities above 95% and specificities above 85%); indeed, quantitative versions of the reverse-transcription and polymerase chain reaction (RT-qPCR) amplification methods are the gold standard for diagnostics for SARS-CoV-2 infection [2]. However, the feasibility of massive testing using RT-qPCR has been seriously challenged by COVID-19. Alternative amplification methods (strategies based mainly on Loop-mediated amplification methods (LAMP)) may enable accurate and massive SARS-CoV-2 detection (even from saliva) during the first 11 days of infection [9,10]. The methods based on the detection of anti-SARS-CoV-2 antibodies in blood (or serological methods) are poorly suited for diagnosis of infection during the first two weeks [11]. However, they are precisely suitable for evaluating the immune reaction to SARS-CoV-2 infection in a subject (whether symptomatic or asymptomatic) after 14 days of infection.

Massive worldwide serological testing is needed to determine the relevant epidemiological indicators related to COVID-19 infection, including the extent of the exposure, the ratio of symptomatic to asymptomatic infected persons, and the duration and extent of immunity after infection [12–15]. Moreover, as vaccines are developed, tested in animal models and humans, and applied to open populations, we will depend on assays for reliable and quantitative characterization of the immune responses associated with the administration of a vaccine to determine the level of immunization conferred [12,16].

Fortunately, the time kinetics of the various immunoglobulins (IgAs, IgMs, and IgGs) produced against SARS-CoV-2 in COVID-19 patients has been well described in recent reports [17]. For instance, we know that the determination of IgGs 15 days after viral exposure is a good indicator of a previous infection. Several semi-automated serological assays are commercially available to determine the likelihood of infection [11,18,19]. Most established commercial platforms perform well, in terms of accurate prediction of infection in convalescent patients, when the analysis is performed 15 days (or more) after a possible contact [19]. However, despite this reliability, automated serological platforms are expensive when compared to other techniques, such as regular enzyme-linked immunoassays (ELISAs).

ELISAs continue to be the most reliable and widely used method for characterization of the amount of antibodies developed against a specific antigen [19,20]. Laboratories around the world, and particularly in developing countries, depend on traditional ELISAs to conduct widespread serological testing. Therefore, reliable and cost-effective antigens for ELISA testing are greatly needed.

In the context of COVID-19 research, a limited number of reports have been published on the development and characterization of SARS-CoV-2 antigens for ELISAs [21–24]. The spike protein (S) [25,26] and the nucleocapsid protein (N) [27] of SARS-CoV-2 have been used for COVID-19 serological diagnostics [22]. However, only a few detailed reports have been made available on the characterization of ELISAs for the identification of anti-SARS-CoV-2 antibodies [5,15,21,22]. Most of these reports describe transient mammalian cell expression [21,23,28] of the entire spike protein of SARS-CoV-2, or a fraction of the spike protein containing the RBD or receptor-binding domain [28].

Here, we report the production of an antigen inspired by the structure of the receptor-binding domain (RBD) [28] of the spike protein of SARS-CoV-2. This antigen is produced by a bacterial culture of *Escherichia coli*, which enables massive production at low cost [29]. In addition, we characterize and contrast the performance of two ELISA versions, involving (a) direct attachment of the antigen to the surface of plates or (b) the use of a bed of anti-histidine antibodies (anti-his-mediated ELISA) to engineer the reactive surface.

2. Materials and Methods

2.1. Design of S-RBD$_{N318-V510}$ and Prediction of Its 3D Structure

We used the Geneious 11.1.5 software (Biomatters, Ltd., Auckland, New Zealand) to design the vector pFH8-RBD SARS-CoV-2 that contained the RBD (region of 193 aa from N318 to V510) of the SARS-CoV-2 spike protein. The construct also contained a region for the expression of M FH8 [30], an enterokinase restriction site, as well as a histidine tag (his-tag). Histidine and FH8 tags were added for use in the purification process. The histidine tag (his-tag) provides an additional handle for separation using his-tag affinity columns (loaded with divalent ions such as Ni^{+2}). In addition, antigenic proteins containing histidine tags can be fixed to surfaces through anti-histidine antibodies to enable ELISA serological assays using his-tagged antigens [29,31].

The 3D structure of the RBD protein with tags was predicted using the software I-TASSER server (University of Michigan, Ann Arbor, MI, USA).

Figure 1a schematically shows the sequence that we used to encode and produce the MFH8-RBD$_{Spike}$-HisTag protein (S-RBD$_{N318-V510}$ for short). This expression cassette was inserted in a plasmid for expression in *E. coli*. Figure 1c shows the molecular 3D structure of this product, as predicted by molecular structure simulations.
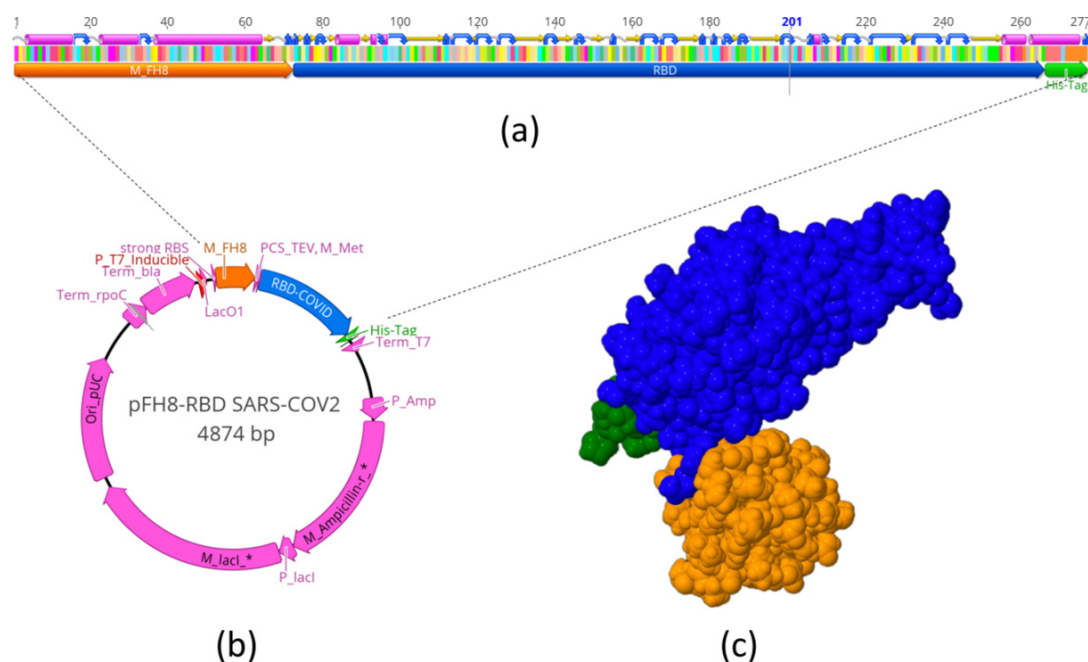

Figure 1. Expression of S-RBD$_{N318-V510}$ in *Escherichia coli*. (**a**) Schematic representation of the sequence used to produce the MFH8-RBD$_{Spike}$-HisTag protein (S-RBD$_{N318-V510}$). This expression cassette was inserted into the (**b**) pFH-RBD SARS-CoV-2 plasmid for expression in *E. coli*. (**c**) Molecular 3D structure of the S-RBD$_{N318-V510}$ protein, as predicted by molecular structure simulations.

2.2. Cloning and Transformation

The full spike coding sequence was synthesized by GenScript (Piscataway, NJ, USA) and was used to obtain the sequences comprising the RBD. This sequence was cloned in an expression vector (ATUM, Newark, CA, USA) regulated by a T7 promoter (IPTG-inducible) using a SapI restriction site and T4 DNA ligase (New England Biolabs, Ipswich, MA, USA). The expression vector was transformed into chemical-competent *E. coli* BL21 strain C41 cells (Lucigen Corporation, Middleton, WI, USA) to obtain producer clones. High-producer clones were further cultured using Luria–Bertani (LB) medium in Erlenmeyer flasks, and recombinant expression was induced using isopropyl β-d-1-thiogalactopyranoside (IPTG).

2.3. RBD Production in Erlenmeyer Flasks

The highest-producer clone was selected and cultured in Luria–Bertani broth containing 50 µg/mL ampicillin (LB-Amp) in 2 L Erlenmeyer flasks. For the initial growth, 200 mL of LB-Amp broth was maintained overnight at 37 °C with 250 rpm agitation in an orbital shaker (VWR International, Radnor, PA, USA). After 12 h of culture, cells were harvested using a Z36 HK centrifuge (Hermle Labortechnik, Wehingen, Germany) at $5000\times g$ for 10 min. The cell pellet was then resuspended in fresh LB-Amp broth containing 1 mM isopropyl β-d-1-thiogalactopyranoside (IPTG) to induce RBD production. The induction was conducted at 30 °C with agitation at 250 rpm for 8–12 h. After induction, cells were recovered by centrifugation at $5000\times g$ for 10 min at 4 °C. Cell pellets were kept at −20 °C until further processing.

2.4. S-RBD$_{N318-V510}$ Recovery and Purification

Pellets from IPTG-induced cells were re-suspended in phosphate-buffered saline (PBS) (pH = 7.4) containing 100 mM NaCl in a proportion of 7.5 mL per gram of cells (wet weight). The cells were then disrupted in an EmulsiFlex-C3 high-pressure homogenizer (Avestin, Ottawa, ON, Canada). The process comprised three cycles, with the first cycle set to reach 5000 psi and the following two cycles performed at 20,000 psi. Cell lysates were centrifuged at $15,000\times g$ for 30 min at 4 °C in a Z36 HK centrifuge. The pellet containing the inclusion body (IB) was re-suspended in IB wash buffer (PBS, pH = 7.4, 1mM EDTA, 500 mM NaCl, 2 M urea, and 2% Triton X-100) at a ratio of 25 mL per g of IB pellet (wet weight), centrifuging to recover the pellet, washing with PBS, and re-suspending in IB solubilization buffer (PBS, pH = 8.0, 500 mM NaCl, 8 M Urea, 2.5 mM 2-mercaptoethanol, and 10 mM imidazole).

The S-RBD$_{N318-V510}$ protein was purified by immobilized metal-affinity chromatography (IMAC), using a HiTrap™ column (GE Healthcare, UK) packed with 1 mL Ni^{2+} charged agarose Ni-NTA Superflow (Quiagen, Germany) in an Akta Pure system (GE Healthcare, Chicago, IL, USA) chromatography system. The degree of purity of S-RBD$_{N318-V510}$ was estimated from SDS-PAGE protein profiles using Image J, an open source software for scanning densitometry analysis.

A dual-phase separation strategy was implemented. Phase A consisted of 20 mM PBS, 300 mM NaCl, and 20 mM imidazole, pH = 7.4, and phase B was 20 mM PBS, pH = 7.4, 300 mM NaCl, and 300 mM imidazole at pH = 7.4. The purification protocol was set with an initial equilibrium of 10 column volumes (CV) of phase A and a flow rate of 1 mL/min. A 5 mL sample of protein was injected at a flow rate of 0.5 mL/min. After sample injection, a washing step of 8 CV was set at a flow rate of 1 mL/min, followed by elution with 3 CV of a linear gradient from 0% to 80% of phase B, then 10 CV of 20%/80% phase A/B, and finally 5 CV of 100% phase B, all at a flow rate of 1 mL/min. Finally, to prepare for further purifications, the column was re-equilibrated with 5 CV of phase A at 1 mL/min. The fraction containing the protein of interest was recovered based on the chromatogram and stored at 4 °C.

2.5. ELISA Assays

We developed and characterized two ELISA strategies/formats for the evaluation of presence of specific anti-SARS-CoV-2 antibodies (Figure 2a,b). Standard commercial 96-well micro-assay plates (CorningH, Maxisorp™; Waltham, MA, USA) were used.

In the first format, 100 µL of 1 µg/mL RBD in PBS was dispensed into each well and incubated for 8 h at 4 °C, followed by addition of 100 µL 5% skim milk in PBS and further incubation for 1 h at room temperature, and then three washes with PBS containing 0.05% Tween-20™. Rabbit anti-spike-SARS-CoV-2 pAb (100 µL; 1:2000 dilution; Sino Biological Inc., Wayne, PA, USA) was then added incubated for 1 h at room temperature, followed by three washes with PBS containing 0.05% Tween-20™. The presence of rabbit antibodies was revealed by adding donkey anti-rabbit-HRP (100 µL, 1:5000 dilution; Pierce, Rockford, IL, USA), followed by three washes with PBS containing 0.05% Tween-20™.
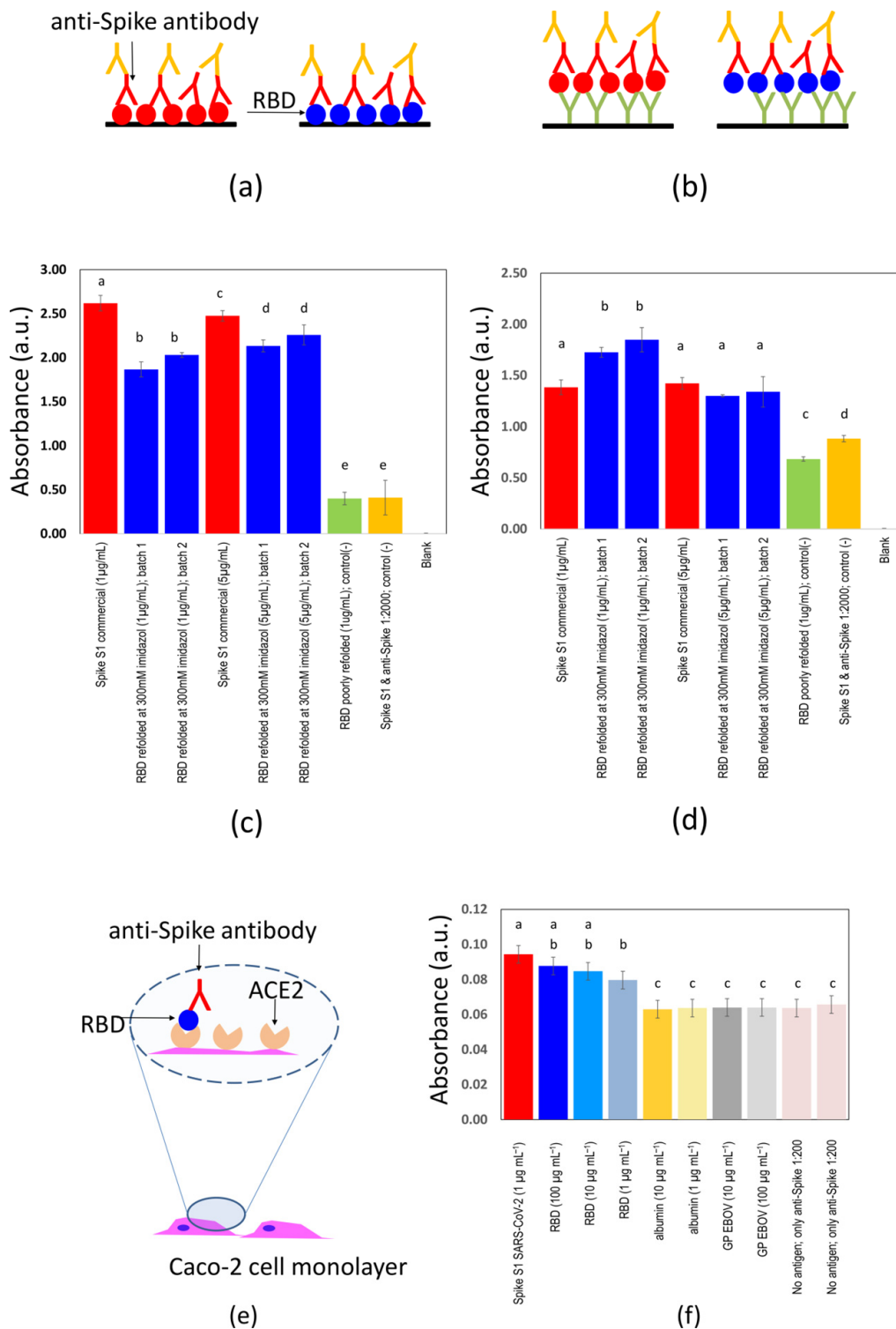
Figure 2. Contrast of two versions of ELISAs for identification of anti-spike SARS-CoV-2 antibodies. Comparison of a commercial full-length spike protein from SARS-CoV-2 (red circles) and the S-RBD$_{N318-V510}$ protein (blue circles) produced in *Escherichia coli* as antigens in ELISA experiments performed to identify anti-spike SARS-CoV-2 antibodies. The antigen was (**a**) directly bound to the surface of 96-well plates, or (**b**) bound through a layer of anti-histidine antibodies (red Ys). In both cases, the specific attachment of anti-spike SARS-CoV-2 antibodies (blue Ys) was revealed by binding of anti-human heavy-chain antibodies functionalized with horseradish peroxidase (yellow Ys). Comparison of absorbance readings for (**c**) direct ELISAs or (**d**) anti-histidine-mediated ELISAs. A commercial full-length spike (red bars) or the S-RBD$_{N318-V510}$ protein (blue bars) was used as the antigen. Commercially available anti-spike SARS-CoV-2 antibodies were used as reactants. Negative controls consisted of the S-RBD$_{N318-V510}$ protein either deficiently folded in glycerol and phosphate-buffered saline

(PBS) (green) or properly folded S-RBD$_{N318-V510}$ antigen in a highly diluted solution (1:20,000) of commercial anti-spike S1 antibodies (yellow). A blank control, where only PBS is added, was also included (absorbance reading ~0.0). (**e**) The specific binding between S-RBD$_{N318-V510}$ and the angiotensin-converting enzyme 2 (ACE2) was determined in experiments with Caco-2 cell monolayers. (**f**) Absorbance reading in ELISA experiments where Caco-2 cell monolayers were incubated with different solutions containing commercial spike protein (red bars) or varying concentrations of the S-RBD$_{N318-V510}$ protein (blue bars). The retention of the antigen on the surface of the Caco-2 cells was evidenced by the subsequent addition of commercial rabbit anti-spike pAb and donkey anti-rabbit-HRP pAb solutions, and the detection of the HRP (as described in Section 2, Materials and Methods). Negative controls containing albumin (yellow bars), recombinant glycoprotein (GP) from the Ebola virus (gray bars), and only anti-spike rabbit pAb (pink bars) were included. Letters indicate statistically different groups ($p < 0.05$; Tukey's test).

The horseradish peroxidase (HRP) was then detected by adding 100 μL 1-Step^{TM} Ultra TMB-ELISA (Pierce, Rockford IL, USA) until a blue color was observed. The reaction was stopped by adding 100 μL 1M H$_2$SO$_4$, and the absorbance was measured at 450 nm in a BioTek microplate reader (Winooski, VT, US).

The second ELISA format consisted of first sensitizing the plate wells with mouse anti-histidine pAb (100 μL, 1:1000 dilution; Bio-Rad Laboratories, Inc., Hercules, CA, USA) and incubating for 8 h at 4 °C, then blocking with skim milk for 1 h at room temperature, followed by three washes with PBS containing 0.05% Tween-20^{TM}. The plates were then incubated with RBD for 1 h at room temperature. All subsequent steps were as described for the first ELISA format.

2.6. ELISA Testing of Serum Samples

We performed ELISA experiments using samples of sera from non-exposed individuals and convalescent, positive volunteers. Five samples of sera from COVID-19 non-exposed individuals were collected from volunteers at Hospital San José (Nuevo León, México), from June 2009 to October 2009, during pandemic Influenza A/H1N1/2009. Fifty-five samples of sera from convalescent patients previously confirmed as COVID-19 (+) by RT-qPCR were collected at Alfa Medical S.A. de C.V. (Monterrey, N.L., México). Samples were collected from patients after obtaining informed and signed written consent and in complete observance of good clinical practices, the principles stated in the Helsinki Declaration, and applicable lab operating procedures at Hospital Alfa. Every precaution was taken to protect the privacy of sample donors and the confidentiality of their personal information. The experimental protocol was approved on 20 May 2020 by a named institutional committee (Alfa Medical Center, Research Committee; resolution AMCCI-TECCOVID-001).

Two different ELISA strategies were contrasted. In the first format (direct ELISA), 100 μL of 1 μg/mL RBD in PBS was dispensed into each well of 96-well plates and incubated for 8 h at 4 °C, followed by blocking with 100 μL 5% skim milk in PBS and incubation for 1 h at room temperature, and three washes with PBS containing 0.05% Tween-20^{TM}. Different dilutions (1:5, 1:50, 1:100, and 1:200; 100 μL) of serum from volunteers were added per well, incubated for 1 h at room temperature and then washed three times with PBS containing 0.05% Tween-20^{TM}. The best results were observed when 1:100 dilutions were used. The presence of human IgG was detected by adding goat anti-human IgG HRP (100 μL; 1:10,000 dilution; Pierce Biotechnology Inc., Rockford, IL, USA) and incubating for 1 h at room temperature, followed by three washes with PBS containing 0.05% Tween-20^{TM} and detection with 1-Step^{TM} Ultra TMB-ELISA.

In the second format (sandwich ELISA), RBD (100 μL; 1 μg/mL in PBS) was dispensed in each well and incubated for 1 h at room temperature followed by three washes with PBS containing 0.05% Tween-20^{TM}. Then 100 μL of different dilutions (1:5, 1:50, 1:100, and 1:200) of serum from volunteers were added per well, incubated for 1 h at room temperature and subsequently washed three times with PBS containing 0.05% Tween-20^{TM}. The presence of human IgG was again detected with goat anti-human IgG HRP, and the remaining steps were conducted as described for the first ELISA format.

2.7. Binding between S-RBDN$_{318-V510}$ Protein and the ACE2 Receptor in Caco-2 Cells

We conducted experiments in Caco-2 cells (ATCC® HTB-37) to assess the specific binding between S-RBD$_{N318-V510}$ and the angiotensin-converting enzyme 2 (ACE2). Toward that aim, we established monolayer cultures of Caco-2 cells in 96-well plates. At confluence, culture medium was removed, and cells were covered with paraformaldehyde, incubated for 10 minutes at room temperature for fixation, added with 100 µL 5% skim milk in PBS, further incubated for 1 h at room temperature, and washed three times with PBS containing 0.05% Tween-20™. Subsequently, 100 µL of a solution of RBD in PBS were added to the fixed cell monolayer. Three different RBD concentrations were assayed (i.e., 1, 10, and 100 µg/mL). Albumin and glycoprotein (GP) from the Ebola virus were used as negative controls. All proteins were incubated on the Caco-2 monolayer for 1 h at room temperature and then washed three times with PBS containing 0.05% Tween-20™. A rabbit anti-spike-SARS-CoV-2 pAb (100 µL; 1:1000 dilution; Sino Biological Inc., PA, USA) was then added and incubated for 1 h at room temperature, followed by three washes with PBS containing 0.05% Tween-20™. The presence of rabbit antibodies was revealed by adding donkey anti-rabbit HRP (100 µL, 1:10,000 dilution; Pierce, Rockford, IL, USA), followed by three washes with PBS containing 0.05% Tween-20™. HRP was detected by adding 100 µL 1-Step™ Ultra TMB-ELISA (Pierce, Rockford, IL, USA) until blue was observed. The reaction was stopped by adding 100 µL 1M H_2SO_4, and the absorbance was measured at 450 nm in a BioTek microplate reader (VT, US).

2.8. Antigenicity Assessment of Peptide S-RBD$_{N318-V510}$ in Mice

We explored the use of peptide S-RBD$_{N318-V510}$ as an antigen in a reduced set of in vivo experiments in mice. We subcutaneously injected six mice with 20 µg of the purified peptide S-RBD$_{N318-V510}$ dissolved in HEPES. Three mice was used as a negative control (i.e., injected with only HEPES). We collected blood from the tails of our animals 14 days after injection and then conducted ELISA experiments using the scheme of ELISAs mediated by the use of a layer of anti-histidine antibodies.

This experiment complied with the 3Rs (replacement, reduction, and refinement) in animal model research. The experimental scheme was approved by the Research and Ethics Committee of Alpha Medical Center, at Nuevo-León, México (Approval AMCCI-TECOVID-001; 12 May 2020). To honor the lives of these animals, their sera were used not only to establish the efficacy of the peptide S-RBD$_{N318-V510}$ as an antigen for serological testing but also its potential as an ingredient for vaccines. These results will be presented in a follow-up report.

3. Results

3.1. Antigen Production and Purification

We engineered an expression construct for the recombinant production of the RBD of the S protein of SARS-CoV-2. Specifically, we selected the region of the S-RBD between the residues N318 and V510 of the consensus sequence of the S protein of SARS-CoV-2.

Reproducible productions of up to 2 g (dry weight) of biomass L^{-1} was obtained in 2 L Erlenmeyer flasks incubated in orbital shakers at 30 °C for 12 h. At this point, this production process has not yet been scaled up to an instrumented bioreactor. However, based on our previous work with other antigens expressed in bacterial systems, we anticipate that this scale-up will further increase biomass production to 10–20 g L^{-1} [32]. The methods described here (Section 2, Materials and Methods) lead to the production of S-RBD$_{N318-V510}$ in inclusion bodies (IBs); we found negligible amounts of the protein in the supernatant of *E. coli* cultures. We implemented a conventional separation purification protocol that included lysis in a high-throughput homogenizer, filtration, re-suspension, and purification using his-tag columns.

After lysis, different refolding and purification strategies were tested, including the use of different columns and combinations of resuspension buffers and conditions. The best results were obtained by suspending the cell pellet in IB washing buffer at a ratio

of 25 mL per g of IB pellet (wet weight), centrifuging to recover the pellet, washing with PBS, and re-suspending in IB solubilization imidazole-based buffer. The S-RBD$_{N318-V510}$ protein was then purified by immobilization metal-affinity chromatography in a preparative chromatography system. After testing different purification protocols, we opted for a two-phase purification protocol (as described in Section 2, Materials and Methods).

Western blots conducted using marked anti-histidine antibodies indicated that the recombinant product was produced and could be purified with sufficient yield and purity by the methods described here. The molecular weight of the S-RBD$_{N318-V510}$ protein (approximately 31 kDa) was consistent with the expected value. The degree of purity of the RBD was estimated at approximately 92% based on the SDS-PAGE protein profiles and using the Image J open-source software for scanning densitometry analysis. We have consistently obtained overall yields of approximately 1.5 mg of pure S-RBD$_{N318-V510}$ per liter of culture medium among different batches.

3.2. Determination of Binding Affinity

We evaluated the binding affinity of the S-RBD$_{N318-V510}$ protein in two sets of ELISA experiments using commercial anti-RBD antibodies. In the first set of experiments (direct ELISAs; Figure 2a), we directly deposited 1 μg of purified S-RBD$_{N318-V510}$ per well in 96-well plates. We then added a commercial anti-S(RBD) antibody to each well, and the relative amount of antibody bound to S-RBD$_{N318-V510}$ protein was determined by absorbance after the addition of an anti-heavy-chain antibody marked with horseradish peroxidase (HRP). The S-RBD$_{N318-V510}$ protein exhibited a binding affinity of approximately 75.51% $\pm$ 5% of that of the commercial control (Figure 2c).

Importantly, our construct contained a histidine tag (his-tag). Antigenic proteins containing histidine tags can be fixed to surfaces through anti-histidine antibodies to enable ELISA serological assays using his-tagged antigens [29,31]. In a second set of experiments, we conducted sandwich-type ELISAs (Figure 2b). For that purpose, the S-RBD$_{N318-V510}$ protein was bound to the bottom surface of the 96-well plates through an anti-histidine antibody [29]. In concept, this strategy may promote a more uniform orientation of the S-RBD$_{N318-V510}$ protein and thereby improve the selectivity of the assay. Indeed, the binding ability of S-RBD$_{N318-V510}$ protein was 26.63% $\pm$ 5% higher than that shown by the commercially available spike protein used here as a positive control (Figure 2d).

In addition, we conducted experiments in which we exposed Caco-2 cells to S-RBDN$_{318-V510}$. With these experiments (Figure 2e,f), we assessed the specific binding between S-RBDN$_{318-V510}$ and the angiotensin-converting enzyme 2 (ACE2). ACE2 is the natural receptor of the spike protein [33]) in human cells and is natively present on the surface of Caco-2 cells [34,35].

3.3. Determination of Binding Affinity Using Human and Animal Sera

We ran an additional series of ELISA experiments using actual human sera and contrasted the results with those of the two ELISA versions previously discussed.

In a first round of experiments, we directly bound commercial spike protein or S-RBD$_{N318-V510}$ protein to 96-well ELISA plates. First, we used five serum samples from non-exposed individuals collected from June to December 2009 during the first wave of pandemic Influenza A/H1N1/2009 in México. The average absorbance value exhibited by samples of these non-exposed individuals was 0.272 (99% CI 0.243 to 0.301) in ELISAs conducted using the S-RBD$_{N318-V510}$ protein. Similarly, the average absorbance value for non-exposed individuals when the whole spike protein was used was 0.198 (99% CI 0.168 to 0.224). Sera from non-exposed individuals exhibited low absorbance values and enabled the definition of an average reliable absorbance value for non-exposed individuals (first two bars in Figure 3a).
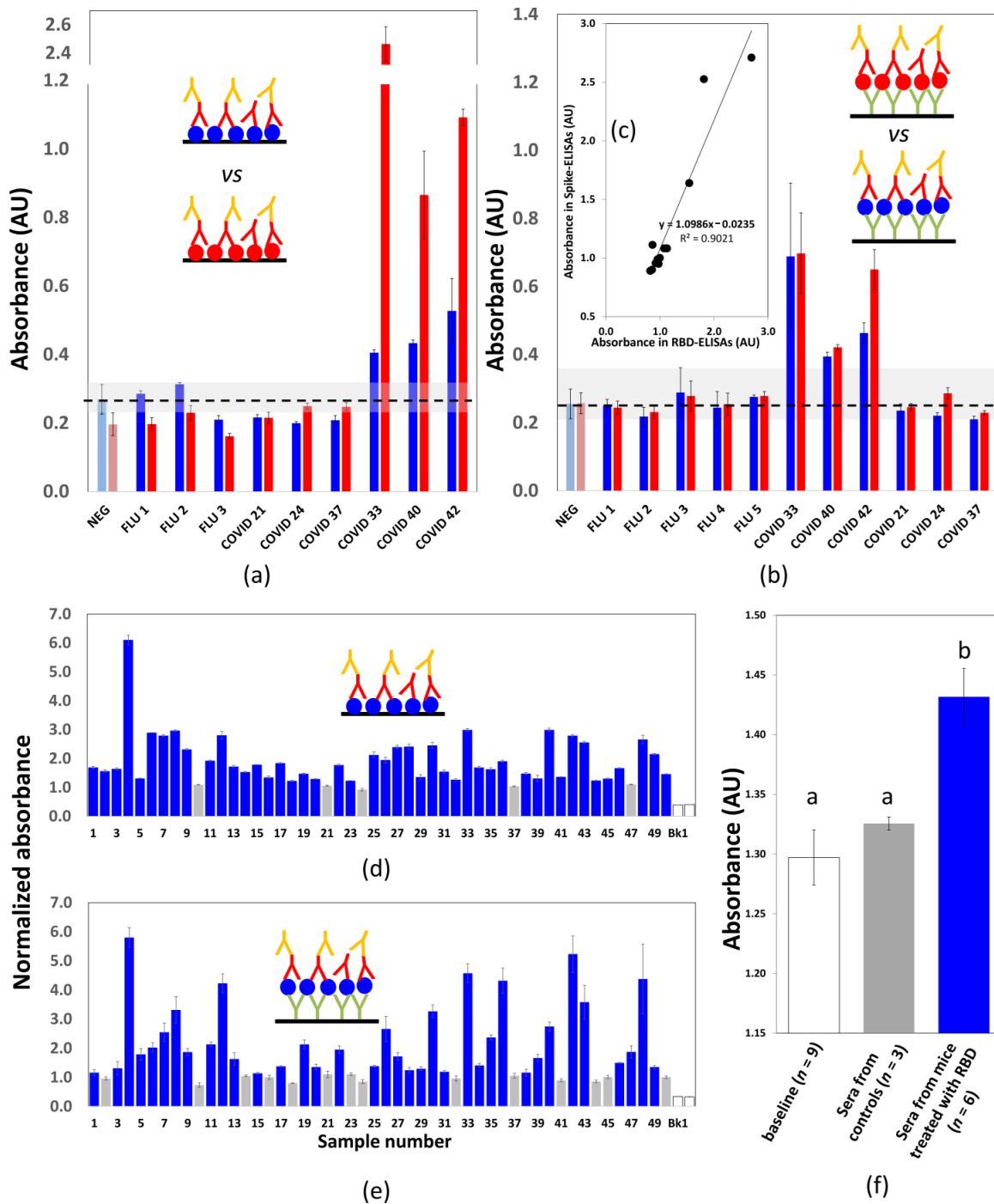
Figure 3. Binding of antibodies from human sera to S-RBD$_{N318-V510}$ using direct and anti-histidine-mediated ELISAs. (**a**) Binding of antibodies from human sera, measured as absorbance readings, in direct ELISA experiments that used a commercial full-length spike (red bars) or the S-RBD$_{N318-V510}$ protein (blue bars) as antigens. Serum samples were obtained from non-exposed volunteers (FLU X; collected during pandemic Influenza A/H1N1/2009) and from volunteers possibly exposed to SARS-CoV-2 (COVID X; collected during pandemic COVID-19). NEG bars indicate the average absorbance reading exhibited by serum samples from non-exposed volunteers. (**b**) Binding of antibodies from human sera, measured as absorbance readings, in anti-histidine mediated ELISA experiments that used a commercial full-length spike (red bars) or the S-RBD$_{N318-V510}$ protein (blue bars) as antigens. Serum samples were obtained from non-exposed volunteers (FLU X; collected during pandemic Influenza A/H1N1/2009) and from volunteers possibly exposed to SARS-CoV-2 (COVID X; collected during pandemic COVID-19). NEG bars indicate the average absorbance reading exhibited by serum samples from non-exposed volunteers. (**c**) Graphic analysis of the correlation between titers obtained in anti-histidine-mediated ELISAs that used the commercial full-length spike (red bars) or the S-RBD$_{N318-V510}$ protein (blue bars) as antigens. All experiments

were conducted using 1:100 serum dilutions. (**d**,**e**) Binding of S-RBDN$_{318-V510}$ serum samples donated by convalescent patients confirmed as COVID-19 (+) by RT-qPCR. Normalized absorbance readings related to the binding affinity of the S-RBD$_{N318-V510}$ protein to human sera antibodies from COVID-19 convalescent patients for (**d**) direct, and (**e**) anti-histidine mediated ELISAs. All absorbance readings were normalized by the average absorbance reading exhibited by samples from non-exposed individuals. Normalized readings higher than the threshold value of 1.11 (for direct ELISAs) or 1.12 (for anti-histidine-mediated ELISAs) are indicated in blue. Absorbance readings from blanks (phosphate-buffered saline only) are indicated in yellow as a reference. Experiments were conducted using 1:100 serum dilutions. (**f**) Absorbance readings related to the binding affinity of the S-RBD$_{N318-V510}$ protein to sera antibodies from mice subcutaneously inoculated with S-RBD$_{N318-V510}$ 14 days before (blue bars) and to control animals (injected only with vehicle (i.e., HEPES; gray bar). Absorbance readings related to the complete set of mice before injection (at day 0; white bar). Letters indicate statistically different groups ($p < 0.05$; Tukey's test).

Figure 3a shows the absorbance readings from direct ELISA experiments conducted on a set of selected serum samples. In this set, we included sera from non-exposed COVID-19 individuals (the samples collected in 2009). We also selected samples from probably exposed individuals that exhibited absorbance values statistically similar to negative samples, as well as sera from convalescent patients diagnosed as COVID-19 (+) by RT-qPCR. The performance of the S-RBD$_{N318-V510}$ protein (blue bars) and a commercial spike protein (magenta bars) was compared. Some of the samples exhibited values that exceeded the thresholds of the 99.5% confidence values for serologically negative samples. Consistently, these samples corresponded to sera from convalescent COVID-19 patients.

Both the full-length commercial spike antigen and the S-RBD$_{N318-V510}$ protein antigen were able to discriminate between samples from non-exposed individuals and COVID-19 (+) patients. However, consistent with recent reports [36], the absorbance values were much higher when the full-length commercial spike protein was used as the ELISA antigen than when the S-RBD$_{N318-V510}$ protein was used. Therefore, in this ELISA format, the difference in absorbance value between positive and negative samples was greater when the spike protein was used than when the S-RBD$_{N318-V510}$ protein is used.

We repeated these ELISA experiments using a second strategy consisting of binding the antigens through a layer of anti-histidine antibodies. Figure 3b shows the results of a parallel ELISA experiment using a layer of anti-histidine antibodies to bind the antigens to the plate surfaces.

The average absorbance value for non-exposed individuals was 0.257 (99% CI 0.237 to 0.277) and 0.255 (99% CI 0.226 to 0.284) for the full-length spike and the S-RBD$_{N318-V510}$ protein, respectively. In general, the absolute values of the absorbance readings were lower in the anti-histidine-mediated ELISAs than in the direct ELISAs. The absorbance readings produced using the full spike and S-RBD$_{N318-V510}$ were remarkably similar (Figure 3b,c). This suggests that the anti-histidine antibodies allow similar arrangement and alignment of both antigens to present reactive surfaces of comparable antibody binding capacity.

We further studied the usefulness of these two ELISA versions (direct or mediated by anti-histidine antibodies) by testing 50 samples from convalescent patients diagnosed as COVID-19 (+) by RT-qPCR. Most of these patients had shown COVID-19-related symptoms at least 7 days before blood collection. Figure 3d,e shows the normalized absorbance readings for this set of serum samples, with no particular order, as determined by ELISA testing conducted by direct sensitization of the reactive surface with S-RBD$_{N318-V510}$. Figure 3e shows results from ELISAs that used an anti-histidine-mediated binding to sensitize the reaction with S-RBD$_{N318-V510}$. The normalization of the absorbance values consisted of dividing the absolute absorbance by the average value of absorbance readings of sera from three non-exposed individuals.

We also established threshold values for normalized absorbance to discriminate between the negative and positive results for threshold values of normalized absorbance of 1.11 and 1.12 for direct and anti-histidine-mediated ELISAs using S-RBD$_{N318-V510}$, respectively. These values were selected to be slightly above the upper threshold of the 99% CI of the average readings of non-exposed individuals.

Finally, we explored the use of peptide S-RBD$_{N318-V510}$ as an antigen in a reduced set of in vivo experiments in mice. We subcutaneously injected six mice with 20 μg of the purified peptide S-RBD$_{N318-V510}$ dissolved in HEPES. We collected blood from the tails of our animals 14 days after injection and then conducted ELISA experiments using the second scheme of ELISAs that we proposed in this manuscript (mediated by the use of a layer of anti-histidine antibodies). We found that six of the six mice produced specific antibodies against S-RBD$_{N318-V510}$, while the absorbance signal remained at the basal level in the control mice (i.e., injected with only HEPES; Figure 3f). This suggests that (a) this peptide is an effective antigen in mice and (b) that the ELISA method that we propose here is also useful for characterizations in immunization experiments.

4. Discussion

Arguably, antigens are one of the most important reagents that clinicians will require while facing COVID-19 pandemics in the months to come. Complete COVID-19 ELISA kits are commercially available, but their cost (approximately 8 USD per reaction, per well) still limits massive implementation, particularly in developing economies. The current value of commercially available S1-derived SARS-CoV-2 antigens is approximately 7 USD μg^{-1}, which is also prohibitive for most laboratories for large-scale screening of COVID-19-seropositive subjects.

Here, we report methods for the production of a portion of the S1 fraction of the SARS-CoV-2 spike protein that contains the receptor-binding domain for the angiotensin II human receptor. We engineered an expression construct for the recombinant production of the RBD of the S protein of SARS-CoV-2. Specifically, we selected the region of the S-RBD between the residues N318 and V510 of the consensus sequence of the S protein of SARS-CoV-2. In a recent report, a similar fraction of the SARS-CoV-2 spike protein (from residues 331 to 510) containing the RBD has been transiently expressed in HEK293 cells [28]. That peptide successfully recognized the ACE receptor, the native target of the RBD of the spike protein [28].

We chose *Escherichia coli* as an expression host, and we describe a straightforward process, amenable to widespread implementation, for the production and purification of the S-RBD$_{N318-V510}$ protein. The fact that our antigen is expressed in bacterial systems greatly facilitates its production and paves the way to scaling up. We show that antigen production of 1.5 mg per L is feasible, even when using non-agitated Erlenmeyer flasks and non-instrumented bioreactors. This production level is already attractive, since production can be completed in 24 h.

However, the use of a bacterial system to express an effective antigen is not always feasible. Bacterial systems lack the capacity to conduct post-translational modifications (e.g., glycosylation), and glycosylation is often required for functionality. Therefore, recombinant proteins produced in bacterial systems may exhibit lower functionality than analogous proteins produced in eukaryotic systems (e.g., CHO or HEK cells).

Here, we investigate whether the S-RBD$_{N318-V510}$ protein, when produced in a bacterial system, still retains its ability to bind anti-RBD antibodies. Our results suggest that this is the case; S-RBD$_{N318-V510}$ performs satisfactorily as an antigen in ELISA assays when compared with commercial versions of the spike protein.

From these results, however, it should not be directly inferred that protein S-RBD$_{N318-V510}$ retains its capability for effective binding to the ACE2 receptor. We conducted experiments in which we exposed Caco-2 cells (a cell line we use routinely in our lab that natively possesses ACE2) to S-RBD$_{N318-V510}$. In parallel experiments, we exposed Caco-2 cells to other proteins (i.e., albumin, a recombinant version of the GP protein from the Ebola virus) to investigate for unspecific attachment. The results of these experiments suggest the specific attachment of S-RBD$_{N318-V510}$ to the ACE2 receptor in Caco-2 cells (Figure 2e,f).

The binding of the S-RBD$_{N318-V510}$ protein to Caco-2 surfaces was significantly higher than that of the anti-spike pAbs to Caco-2 surfaces. Moreover, the binding of S-RBD$_{N318-V510}$ to Caco-2 cells was not dose dependent in the window of concentrations of our experiments

(i.e., 1 to 100 µg mL^{-1}). However, the binding of the full-length spike protein to Caco-2 cells is higher than that of S-RBD$_{N318-V510}$ at the lowest concentration tested (i.e., 1 µg mL^{-1}). At higher concentrations of S-RBD$_{N318-V510}$, that is, 10- or 100-fold higher, the binding to Caco-2 cells equals that exhibited by the full-length spike. Altogether, this suggests that the S-RBD$_{N318-V510}$ produced in bacteria retains its ability to bind ACE2 but with a lower affinity than the full-length spike expressed in eukaryotic cells.

We describe two different ELISA formats in our experiments (Figure 2a,b). In a direct format, the S-RBD$_{N318-V510}$ protein is directly attached to the surface of the ELISA plate. In a second format, a layer of anti-histidine antibodies mediates the binding between the plate surface and the antigen. In a series of ELISA experiments, we explored the type of ELISA format and the use of different concentrations of the protein S-RBD$_{N318-V510}$. In these ELISA experiments, we include two controls. The first negative control (green bars) consists of an antigen deficiently folded (in glycerol and PBS). The second negative control consists of the properly folded S-RBD$_{N318-V510}$ antigen but added to a highly diluted solution of commercial anti-spike 1 antibody (1:20,000) to simulate a negative sample. A blank control, where only PBS is added, was also included (absorbance reading ~0.0). The readings obtained from sandwich ELISAs are closer to those obtained when a commercial spike S1 protein is used as antigen. While we believe that the sandwich ELISA will produce similar results to those obtained when commercial antigens are used, the direct ELISA still allows discrimination between samples that contain or do not contain anti-spike antibodies and at a lower cost.

In experiments using human sera from patients possibly exposed to SARS-CoV-2, the results of both ELISA formats were highly consistent (Figure 3a–e). As shown earlier, anti-his-mediated ELISAs yielded similar results, regardless of the use of the full-length spike protein or S-RBD$_{N318-V510}$. Therefore, we assumed that the anti-his-mediated results correlated well with ELISAs conducted with the full spike protein and can be taken as a reference for determining the sensibility and specificity of direct ELISAs performed using S-RBD$_{N318-V510}$. When this is done, the selectivity and specificity of the direct S-RBD$_{N318-V510}$ format are 97.2% and 52.0%, respectively, when a threshold value of normalized absorbance of 1.10 is used. If a threshold value of normalized absorbance of 1.25 is used instead, the values of selectivity and specificity are 97.2% and 68.0%, respectively. The overall accuracy of the direct S-RBD$_{N318-V510}$ ELISA test (i.e., the overall consistency of the results with respect to the anti-his S-RBD$_{N318-V510}$ ELISA) was 81.8% and 85.45% when the thresholds were set at 1.10 and 1.25, respectively. Overall, these results suggest that the anti-his S-RBD$_{N318-V510}$ ELISA is more consistent with full-length spike ELISAs. However, direct S-RBD$_{N318-V510}$ ELISA can be used in serological testing (further reducing the cost) with only a minimum sacrifice of selectivity but with an increased probability of false positives.

5. Conclusions

Here we report protocols for the recombinant production of the protein S-RBD$_{N318-V510}$, a short peptide of ~33 kDa inspired by the receptor binding domain of the spike protein of SARS-CoV-2, in bacterial systems. We cloned the construct for the production of S-RBD$_{N318-V510}$ in *E. coli* BL21 strain C41. Moreover, we demonstrate that a simple purification method, based on the use of his-tag-mediated affinity chromatography and refolding using imidazole solutions, leads to the production of a functional antigen that can be used to discriminate between samples that contain and do not contain anti-spike SARS-CoV-2 antibodies. In ELISA experiments using commercial anti-spike antibodies or actual sera from patients, this protein performs similarly to commercially available antigens based on the expression of larger segments of the spike protein.

Our aim was to enable the widespread use of this simple process to produce a cost-effective SARS-CoV-2 antigen. We believe that a lab-scale manufacturing operation based on the process described here may allow the production of gram amounts per month of an antigen of satisfactory quality to enable wide-scale screening projects in open populations.

This will be particularly useful in the present and near future. Massive serological testing is needed to determine the extent of the exposure to SARS-CoV-2 among regions, the overall ratio of symptomatic to asymptomatic infected persons (which has not been clearly established yet), and the duration and extent of immunity after infection. As the vaccination is deployed, we will also depend on anti-SARS-CoV-2 antibody assays for the reliable, scalable, and cost-effective quantification of the extent of immunity conferred to populations.

Institutional Review Board Statement: The study was conducted according to the guidelines of the Declaration of Helsinki, and approved by the Ethics Committee of Alfa Medical Center (protocol code AMCCI-TECCOVID-001; approved on 20 May 2020).

Informed Consent Statement: Informed consent was obtained from all subjects involved in the study.

Data Availability Statement: The data, central to support in this study, are available in the body of the manuscript and Figures 1–3. Additional raw data relevant to this study and/or related to clinical samples are available on request from the corresponding author. The clinical data are not publicly available due to ethical reasons related to the preservation of the privacy of volunteers.

Conflicts of Interest: The authors declare no conflict of interest. The funders had no role in the design of the study; in the collection, analyses, or interpretation of data; in the writing of the manuscript, or in the decision to publish the results.

References

1. Home—Johns Hopkins Coronavirus Resource Center. (n.d.) Available online: https://coronavirus.jhu.edu/ (accessed on 10 September 2020).
2. Ravi, N.; Cortade, D.L.; Ng, E.; Wang, S.X. Diagnostics for SARS-CoV-2 detection: A comprehensive review of the FDA-EUA COVID-19 testing landscape. *Biosens. Bioelectron.* **2020**, *165*, 112454. [CrossRef] [PubMed]
3. González-González, E.; Santiago, G.T.; Lara-Mayorga, I.M.; Martínez-Chapa, S.O.; Alvarez, M.M. Portable and accurate diagnostics for COVID-19: Combined use of the miniPCR thermocycler and a well-plate reader for SARS-CoV-2 virus detection. *PLoS ONE* **2020**, *15*, e0237418. [CrossRef] [PubMed]
4. González-González, E.; Lara-Mayorga, I.M.; Rodríguez-Sánchez, I.P.; Zhang, Y.S.; Martinez-Chapa, S.O.; de Santiago, G.T.; Alvarez, M.M. Colorimetric Loop-mediated Isothermal Amplification (LAMP) for cost-effective and quantitative detection of SARS-CoV-2: The change in color in LAMP-based assays quantitatively correlates with viral copy number. *Anal. Methods* **2020**. [CrossRef]
5. Amanat, F.; Stadlbauer, D.; Strohmeier, S.; Nguyen, T.H.O.; Chromikova, V.; McMahon, M.; Jiang, K.; Arunkumar, G.A.; Jurczyszak, D.; Polanco, J.; et al. A serological assay to detect SARS-CoV-2 seroconversion in humans. *Nat. Med.* **2020**, *26*, 1033–1036. [CrossRef] [PubMed]
6. Scohy, A.; Anantharajah, A.; Bodéus, M.; Kabamba-Mukadi, B.; Verroken, A.; Rodriguez-Villalobos, H. Low performance of rapid antigen detection test as frontline testing for COVID-19 diagnosis. *J. Clin. Virol.* **2020**, *129*, 104455. [CrossRef] [PubMed]
7. Albert, E.; Torres, I.; Bueno, F.; Huntley, D.; Molla, E.; Fernández-Fuentes, M.Á.; Martínez, M.; Poujois, S.; Forqué, L.; Valdivia, A.; et al. Field evaluation of a rapid antigen test (Panbio^TM COVID-19 Ag Rapid Test Device) for COVID-19 diagnosis in primary healthcare centers. *Clin. Microbiol. Infect.* **2020**. [CrossRef]

8. Diao, B.; Wen, K.; Zhang, J.; Chen, J.; Han, C.; Chen, Y.; Wang, S.; Deng, G.; Zhou, H.; Wu, Y. Accuracy of a nucleocapsid protein antigen rapid test in the diagnosis of SARS-CoV-2 infection. *Clin. Microbiol. Infect.* **2020**. [CrossRef]

9. Thi, V.L.D.; Herbst, K.; Boerner, K.; Meurer, M.; Kremer, L.P.; Kirrmaier, D.; Freistaedter, A.; Papagiannidis, D.; Galmozzi, C.; Stanifer, M.L.; et al. A Colorimetric RT-LAMP Assay and LAMP-Sequencing for Detecting SARS-CoV-2 RNA in Clinical Samples. 2020. Available online: http://stm.sciencemag.org/ (accessed on 24 August 2020).

10. Lalli, M.A.; Chen, X.; Langmade, S.J.; Fronick, C.C.; Sawyer, C.S.; Burcea, L.C.; Fulton, R.S.; Heinz, M.; Buchser, W.J.; Head, R.D.; et al. Rapid and extraction-free detection of SARS-CoV-2 from saliva with colorimetric LAMP. *MedRxiv* **2020**. [CrossRef]

11. Nicol, T.; Lefeuvre, C.; Serri, O.; Pivert, A.; Joubaud, F.; Dubée, V.; Kouatchet, A.; Ducancelle, A.; Lunel-Fabiani, F.; le Guillou-Guillemette, H. Assessment of SARS-CoV-2 serological tests for the diagnosis of COVID-19 through the evaluation of three immunoassays: Two automated immunoassays (Euroimmun and Abbott) and one rapid lateral flow immunoassay (NG Biotech). *J. Clin. Virol.* **2020**, *129*, 104511. [CrossRef]

12. Krammer, F.; Simon, V. Serology assays to manage COVID-19. *Science* **2020**, *368*, 1060–1061. [CrossRef]

13. Clarke, C.; Prendecki, M.; Dhutia, A.; Ali, M.A.; Sajjad, H.; Shivakumar, O.; Lightstone, L.; Kelleher, P.; Pickering, M.C.; Thomas, D.; et al. High Prevalence of Asymptomatic COVID-19 Infection in Hemodialysis Patients Detected Using Serologic Screening. *J. Am. Soc. Nephrol.* **2020**, *31*, 1969–1975. [CrossRef] [PubMed]

14. Lerner, A.M.; Eisinger, R.W.; Lowy, D.R.; Petersen, L.R.; Humes, R.; Hepburn, M.; Cassetti, M.C. The COVID-19 Serology Studies Workshop: Recommendations and Challenges. *Immunity* **2020**, *53*, 1–5. [CrossRef] [PubMed]

15. Roy, V.; Fischinger, S.; Atyeo, C.; Slein, M.; Loos, C.; Balazs, A.; Luedemann, C.; Astudillo, M.G.; Yang, D.; Wesemann, D.; et al. SARS-CoV-2-specific ELISA development. *J. Immunol. Methods* **2020**, *484–485*, 112832. [CrossRef] [PubMed]

16. Lipsitch, M.; Kahn, R.; Mina, M.J. Antibody testing will enhance the power and accuracy of COVID-19-prevention trials. *Nat. Med.* **2020**, *26*, 818–819. [CrossRef] [PubMed]

17. Guo, L.; Ren, L.; Yang, S.; Xiao, M.; Chang, D.; Yang, F.; Cruz, C.S.D.; Wang, Y.; Wu, C.; Xiao, Y.; et al. Profiling Early Humoral Response to Diagnose Novel Coronavirus Disease (COVID-19). *Clin. Infect. Dis.* **2020**, *71*, 778–785. [CrossRef] [PubMed]

18. Suhandynata, R.T.; Hoffman, M.A.; Kelner, M.J.; McLawhon, R.W.; Reed, S.L.; Fitzgerald, R.L. Multi-platform Comparison of SARS-CoV-2 Serology Assays for the Detection of COVID-19. *J. Appl. Lab. Med.* **2020**. [CrossRef]

19. van Elslande, J.; Decru, B.; Jonckheere, S.; van Wijngaerden, E.; Houben, E.; Vandecandelaere, P.; Indevuyst, C.; Depypere, M.; Desmet, S.; André, E.; et al. Antibody response against SARS-CoV-2 spike protein and nucleoprotein evaluated by 4 automated immunoassays and 3 ELISAs. *Clin. Microbiol. Infect.* **2020**. [CrossRef]

20. Bastos, M.L.; Tavaziva, G.; Abidi, S.K.; Campbell, J.R.; Haraoui, L.P.; Johnston, J.C.; Lan, Z.; Law, S.; MacLean, E.; Trajman, A.; et al. Diagnostic accuracy of serological tests for covid-19: Systematic review and meta-analysis. *BMJ* **2020**, *370*, 2516. [CrossRef]

21. Alvim, R.G.F.; Lima, T.M.; Rodrigues, D.A.S.; Marsili, F.F.; Bozza, V.B.T.; Higa, L.M.; Monteiro, F.L.; Leitao, I.C.; Carvalho, R.S.; Galliez, R.M.; et al. An affordable anti-SARS-COV-2 spike protein ELISA test for early detection of IgG seroconversion suited for large-scale surveillance studies in low-income countries. *MedRxiv* **2020**. [CrossRef]

22. Zhang, P.; Gao, Q.; Wang, T.; Ke, Y.; Mo, F.; Jia, R.; Liu, W.; Liu, L.; Zheng, S.; Liu, Y.; et al. Evaluation of recombinant nucleocapsid and spike proteins for serological diagnosis of novel coronavirus disease 2019 (COVID-19). *MedRxiv* **2020**. [CrossRef]

23. Johari, Y.B.; Jaffé, S.R.; Scarrott, J.M.; Johnson, A.O.; Mozzanino, T.; Pohle, T.H.; Maisuria, S.; Bhayat-Cammack, A.; Brown, A.J.; Tee, K.L.; et al. Production of Trimeric SARS-CoV-2 Spike Protein by CHO Cells for Serological. *MedRxiv* **2020**. [CrossRef]

24. Esposito, D.; Mehalko, J.; Drew, M.; Snead, K.; Wall, V.; Taylor, T.; Frank, P.; Denson, J.P.; Hong, M.; Gulten, G.; et al. Optimizing high-yield production of SARS-CoV-2 soluble spike trimers for serology assays. *Protein Expr. Purif.* **2020**, *174*, 105686. [CrossRef] [PubMed]

25. Zhang, B.Z.; Hu, Y.F.; Chen, L.L.; Yau, T.; Tong, Y.G.; Hu, J.C.; Cai, J.P.; Chan, K.H.; Dou, Y.; Deng, J.; et al. Mining of epitopes on spike protein of SARS-CoV-2 from COVID-19 patients. *Cell Res.* **2020**, *30*, 702–704. [CrossRef] [PubMed]

26. He, Y.; Zhou, Y.; Wu, H.; Luo, B.; Chen, J.; Li, W.; Jiang, S. Identification of Immunodominant Sites on the Spike Protein of Severe Acute Respiratory Syndrome (SARS) Coronavirus: Implication for Developing SARS Diagnostics and Vaccines. *J. Immunol.* **2004**, *173*, 4050–4057. [CrossRef] [PubMed]

27. Kang, S.; Yang, M.; Hong, Z.; Zhang, L.; Huang, Z.; Chen, X.; He, S.; Zhou, Z.; Zhou, Z.; Chen, Q.; et al. Crystal structure of SARS-CoV-2 nucleocapsid protein RNA binding domain reveals potential unique drug targeting sites. *Acta Pharm. Sin. B* **2020**, *10*, 1228–1238. [CrossRef]

28. Tai, W.; He, L.; Zhang, X.; Pu, J.; Voronin, D.; Jiang, S.; Zhou, Y.; Du, L. Characterization of the receptor-binding domain (RBD) of 2019 novel coronavirus: Implication for development of RBD protein as a viral attachment inhibitor and vaccine. *Cell. Mol. Immunol.* **2020**, *17*, 613–620. [CrossRef]

29. Alvarez, M.M.; López-Pacheco, F.; Aguilar-Yañez, J.M.; Portillo-Lara, R.; Mendoza-Ochoa, G.I.; García-Echauri, S.; Freiden, P.; Schultz-Cherry, S.; Zertuche-Guerra, M.I.; Bulnes-Abundis, D.; et al. Specific Recognition of Influenza A/H1N1/2009 Antibodies in Human Serum: A Simple Virus-Free ELISA Method. *PLoS ONE* **2010**, *5*, e10176. [CrossRef]

30. Costa, S.; Almeida, A.; Castro, A.; Domingues, L. Fusion tags for protein solubility, purification, and immunogenicity in Escherichia coli: The novel Fh8 system. *Front. Microbiol.* **2014**, *5*, 63. [CrossRef]

31. Rodríguez-Martínez, L.M.; Marquez-Ipiña, A.R.; López-Pacheco, F.; Pérez-Chavarría, R.; González-Vázquez, J.C.; González-González, E.; Santiago, G.T.; de León, C.A.P.; Zhang, Y.S.; Dokmeci, M.R.; et al. Antibody Derived Peptides for Detection of Ebola Virus Glycoprotein. *PLoS ONE* **2015**, *10*, e0135859. [CrossRef]

32. Sánchez-Arreola, P.B.; López-Uriarte, S.; Marichal-Gallardo, P.A.; González-Vázquez, J.C.; Pérez-Chavarría, R.; Soto-Vázquez, P.; López-Pacheco, F.; Ramírez-Medrano, A.; Rocha-Pizaña, M.R.; Álvarez, M.M. A baseline process for the production, recovery, and purification of bacterial influenza vaccine candidates. *Biotechnol. Prog.* **2013**, *29*, 896–908. [CrossRef]

33. Walls, A.C.; Park, Y.J.; Tortorici, M.A.; Wall, A.; McGuire, A.T.; Veesler, D. Structure, Function, and Antigenicity of the SARS-CoV-2 Spike Glycoprotein. *Cell* **2020**, *181*, 281–292.e6. [CrossRef] [PubMed]

34. Hoffmann, M.; Kleine-Weber, H.; Schroeder, S.; Krüger, N.; Herrler, T.; Erichsen, S.; Schiergens, T.S.; Herrler, G.; Wu, N.H.; Nitsche, A.; et al. SARS-CoV-2 Cell Entry Depends on ACE2 and TMPRSS2 and Is Blocked by a Clinically Proven Protease Inhibitor. *Cell* **2020**, *181*, 271–280.e8. [CrossRef] [PubMed]

35. Wang, C.; Wang, S.; Li, D.; Wei, D.-Q.; Zhao, J.; Wang, J. Human Intestinal Defensin 5 Inhibits SARS-CoV-2 Invasion by Cloaking ACE2. *Gastroenterology* **2020**, *159*, 1145–1147. [CrossRef] [PubMed]

36. Chen, X.; Li, R.; Pan, Z.; Qian, C.; Yang, Y.; You, R.; Zhao, J.; Liu, P.; Gao, L.; Li, Z.; et al. Human monoclonal antibodies block the binding of SARS-CoV-2 spike protein to angiotensin converting enzyme 2 receptor. *Cell. Mol. Immunol.* **2020**, *17*, 647–649. [CrossRef]